Catalysis Letters
https://doi.org/10.1007/s10562-019-03064-3

Conversion of Dihydroxyacetone to Methyl Pyruvate Catalyzed by Hybrid Molecular Sieves at Low Temperature: A Strategy for the Green Utilization of Glycerol

Qianqian Luo[1] · Tianliang Lu[1,2] · Jun Xu[1] · Xiaomei Yang[2] · Lipeng Zhou[2]

Received: 27 September 2019 / Accepted: 2 December 2019

Abstract

Methyl pyruvate (MPA) was synthesized from dihydroxyacetone (DHA), the oxidation product of glycerol, over Sn-β and TS-1 hybrid molecular sieves at low temperature. Sn-β and TS-1 provide the active sites for conversion of DHA to methyl lactate (MLA) and oxidation of MLA to MPA, respectively. Synergism of Lewis acid sites on Sn-β and TS-1 realize the production of MPA from DHA. After optimization, 71% yield of MPA can be obtained under 50 °C. This is the first report for the synthesis of MPA from DHA directly.

Graphic Abstract

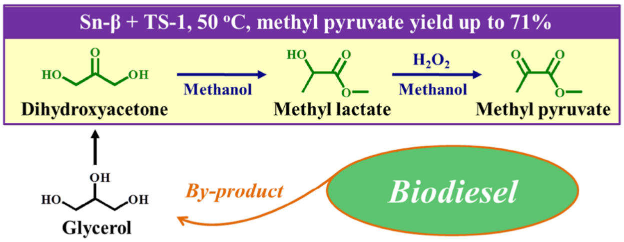

Keywords Catalysis · Biomass conversion · Zeolites · Methyl pyruvate · Dihydroxyacetone

1 Introduction

As important chemicals, pyruvates including pyruvic acid and esters are widely adopted in various fields such as plastic, food, cosmetic, pesticidal, and pharmaceutical industries [1–3]. Meanwhile, applications of pyruvates as raw materials in synthesis of many bioactive substances are attractive [4]. Pyruvates can be produced from tartaric acid by dehydrative decarboxylation. This is the conventional and commercial method for the synthesis of pyruvates. However, excess $KHSO_4$ is used as dehydrating agent in this route resulting in low atom-efficiency and severe environmental pollution. Synthesis of pyruvates can also be realized through carbohydrates fermentation [5], but conditions including temperature, pH value, and so on should be regulated precisely to keep the microbe active. Furthermore, the space time yield of product is low while the separation and purification cost of the product is high. These drawbacks limit the commercialization of this process. Lactates (lactic acid and its esters), the biomass derivates, have similar molecular to pyruvates. For example, the only difference of molecular structure between methyl lactate (MLA) and methyl pyruvate (MPA) is that MLA have 2 more H atoms than MPA. So, preparation of pyruvates from the corresponding lactates by catalytic oxidation attracts much attention due to the excellent atom-efficiency, and various catalysts have been developed [6–13]. Our group had realized the highly

---

✉ Tianliang Lu
lutianliang@zzu.edu.cn

[1] School of Chemical Engineering, Zhengzhou University, 100 Kexue Road, Zhengzhou 450001, People's Republic of China

[2] College of Chemistry, Zhengzhou University, 100 Kexue Road, Zhengzhou 450001, People's Republic of China

efficient synthesis of ethyl pyruvate from ethyl lactate over TS-1 using H_2O_2 as oxidant without solvent, and 97.8% ethyl pyruvate yield can be obtained at 50 °C [13].

Glycerol is the by-product of biodiesel industry. Development of the strategy for the utilization of glycerol attracts much attention from researchers [14–16]. Dihydroxyacetone (DHA) can be obtained from glycerol [17–21]. Xu's group had reported that DHA can be produced from glycerol under mild conditions with high yields. For example, 80% yields of DHA can be offered by Au/CuO at 40–50 °C [21]. Meanwhile, DHA is the precursor for production of lactates which can be further oxidized to pyruvates as mentioned above [22–32]. Thus, realization of direct conversion of DHA to pyruvates under mild conditions is a strategy for the green utilization of glycerol.

Sn containing solid materials [24–32], especially the Sn doped zeolites [27–32], were usually used as catalysts in conversion of DHA to lactates. Our group had prepared hierarchical Sn-USY for this reaction. 100% DHA conversion and higher than 95% MLA yield were obtained at 25–40 °C [32]. Sn-β also shows excellent catalytic performance for the conversion of DHA to lactate [28–31]. Tarnning et al. had investigated the performance of Tin-containing silicates on conversion of DHA to MLA. In the investigated zeolites of Sn-β, Sn-MFI, Sn-MCM-41 and Sn-SBA-15, Sn-β displayed the best performance. Higher than 90% MLA yield achieved at 40 °C [31]. Wang had also applied Sn-β to catalyze the conversion of DHA to MLA, and 92% MLA yield can be obtained at 60 °C [29].

In this work, one-pot conversion of DHA to pyruvate was realized under mild conditions. Based on previous work, Sn containing zeolites was applied as active component for conversion of DHA to lactate, and TS-1 was used to catalyze the conversion of lactate to pyruvate in presence of H_2O_2. After optimization, 100% DHA conversion and 71% MPA yield were obtained at 50 °C over Sn-β and TS-1 hybrid catalyst. This is the first report for the synthesis of MPA from DHA directly.

2 Experimental

2.1 Materials

Zeolites of β and USY were obtained from Nankai University Catalyst Co. (People's Republic of China). DHA, MLA, MPA, and 30% H_2O_2 were purchased from Sinopharm Chemical Reagent Co., Ltd. (People's Republic of China). Tetrabutyl titanate (TBOT), tetrapropylammonium bromide (TPABr), and $SnCl_4{\cdot}5H_2O$ were purchased from Aladdin Chemical Reagent Corporation. Ethanolamine, isopropyl alcohol, naphthalene, colloidal silica, HNO_3, and H_2SO_4 were used as received.

2.2 Synthesis of TS-1

Molar composition of the gel is $n(SiO_2){:}n(TiO_2){:}n(TPABr){:}n(ethanolamine){:}n(H_2O) = 1.0{:}0.033{:}0.1{:}0.5{:}30$. After addition of colloidal Si into the beaker containing ethanolamine, TPABr and H_2O with stirring, TBOT-isopropanol was dropped into the mixture. Then, isopropanol was evaporated. And crystallization of the gel was carried out by hydrothermal treatment at 175 °C for 72 h in a stainless autoclave. After filtration, washing (with H_2O), drying (120 °C, 12 h), and calcination (550 °C, 6 h), white solid of TS-1 was gotten. To make the synthesized TS-1 more stable, further treatment was carried out. The TS-1 was added to the autoclave containing ethanolamine and TPABr. After treatment at 175 °C for 48 h, the TS-1 was separated, and washed with H_2O. Furthermore, the dilute sulphuric acid and hydrogen peroxide solution were used to wash the TS-1. After that, the solid of TS-1 was dried (120 °C, 12 h) and calcined (550 °C, 6 h) for using.

2.3 Synthesis of Sn-β and Sn-USY

The Tin containing zeolites were synthesized by the solid-state ion-exchange method. Take the synthesis of Sn-β as an example. Firstly, Al-β (Si/Al = 13.8) was added to the HNO_3 solution (13 mol L^{-1}) with a solid-to-liquid ratio of 1 g 20 mL^{-1}. After refluxing at 100 °C for 20 h, the solid was separated by centrifugation. Then, the solid was washed by deionized water to neutral. After drying at 100 °C overnight, the obtained solid was transferred to a mortar containing $SnCl_4{\cdot}5H_2O$. The amount of $SnCl_4{\cdot}5H_2O$ was calculated according to the theoretical Sn content of 2 wt%. After grounding for 1 h, the solid was dried at 100 °C overnight. Finally, after calcination at 550 °C for 3 h, the Sn-β was obtained. Sn-USY was also synthesized by this method, but the concentration of HNO_3 solution is 8 mol L^{-1}.

2.4 Catalyst Characterization

Crystalline structures of all the samples were determined by powder X-ray diffraction (XRD) on a Panalytical X'pert PRO instrument. Radiation of Cu Kα ($\lambda = 0.15418$ nm), 40 kV of tube voltage, and 40 mA of tube current were applied in this measurement. Surface area and pore volume were characterized by physical adsorption method on Quantachrome Autosorb. Adsorption/desorption isotherms of N_2 were measured at − 196 °C. Pretreatment of the sample was carried out at 300 °C for 3 h to desorb the H_2O and impurity on the surface. The surface area was calculated by using Brunauer–Emmett–Teller (BET) method. Ti content in TS-1 was measured by a X-ray fluorescence (XRF) spectrometer, and Sn contents in Sn-β and Sn-USY were determined by induced coupled plasma-atomic emission spectroscopy (ICP-AES). UV–Vis spectra of the samples were collected on a Shimadzu UV-2600 spectrophotometer with the wavelength range of 800–200 nm. Bruker Tensor II spectrometer was used to collect the FTIR spectra of the samples with adsorption of pyridine (Pyridine-FTIR). Pretreatment of the sample (9–15 mg) was carried out at 450 °C for 3 h after the analysis pool was evacuated. Then, the spectrum as the background reference was collected at room temperature. The resolution was 4 cm^{-1}. After that, pyridine was introduced to the system to adsorb saturately on the catalyst (about 15 min). Elevate the temperature to desired temperature, and evacuate the system to desorb the pyridine. After evacuation for 30 min, the FTIR spectrum was recorded.

2.5 Catalytic Tests

A round bottom flask with reflux condenser was used as the reactor in this work. Firstly, 0.2 g of DHA along with desired amount of Sn-β and TS-1 were added to the reactor containing 5 mL of methanol under stirring. Then, the reactor was heated to the desired temperature. After reaction for a default time, 30% H_2O_2 was added to the system. Finally, stop the reaction after some hours. Analysis of the reaction mixture was carried out by an Agilent 7890A GC equipped an HP-5 column. Naphthalene was used as the internal standard. The identification of the products was realized by Agilent 6890 N GC/5973 MS and comparison with the authentic samples.

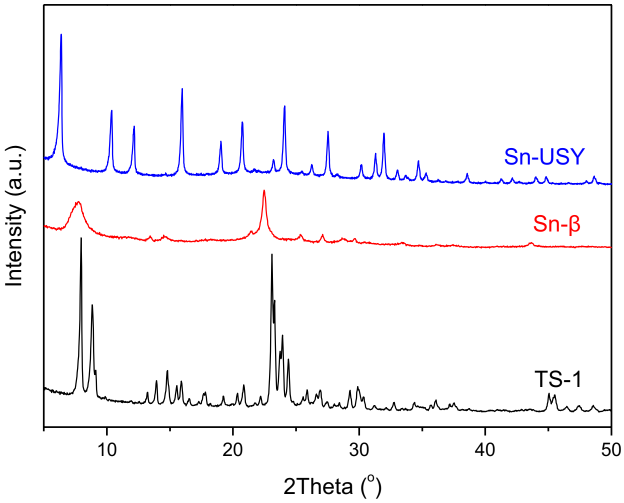

Fig. 1 XRD patterns of TS-1, Sn-β, and Sn-USY

Table 1 Textural properties of the samples

Sample	S_{BET} (m^2 g^{-1})	Total pore volume (mL g^{-1})	$S_{External}$ (m^2 g^{-1})	Mesopore volume (mL g^{-1})
TS-1	380	0.27	45	0.10
Sn-β	435	0.31	98	0.13
Sn-USY	444	0.35	98	0.17

$S_{External}$ $S_{BET} - S_{Micropore}$, *mesopore volume* total pore volume − micropore volume, where the micropore surface area and volume were determined by the *t*-plot method at a relative pressure of 0.05–0.70

3 Results and Discussion

3.1 Catalyst Characterization

Sn-β and Sn-USY were applied for the conversion of DHA to MLA, and TS-1 was used for the oxidation of MLA to MPA. As shown in Fig. 1, XRD patterns confirm the typical BEA structure of Sn-β, FAU of Sn-USY, and MFI of TS-1. As listed in Table 1, all the samples have high total surface area. Both Sn-β and Sn-USY have higher external surface area and mesopore pore volume than TS-1 due to the dealumination procedure for introduction of Sn. Ti content in TS-1 was tested by XRF method, the Si/Ti molar ratio is 31 which is close to the initial Si/Ti molar ratio in the gel for synthesis of TS-1. Sn contents in Sn-β and Sn-USY are 1.91 wt% and 1.88 wt%, respectively, which are close to the theoretical values (2 wt%). Presences of Sn in framework of Sn-β and Sn-USY, and Ti in framework of TS-1 were proved by UV–Vis spectra (Fig. 2). A sharp and intense absorption band at ca. 208 nm is observed in spectra of both Sn-β and Sn-USY. This is usually ascribed to the presence of tetrahedrally coordinated Sn^{IV} [33]. For Sn-β, no obvious band can be observed at around 300 nm, which ascribed to the absorption of SnO_2 as shown in Fig. 2a, implying no aggregated Sn species appeared in synthesis of Sn-β. No difference between spectra of Sn-USY and H-USY can be observed at around 300 nm implying no SnO_2 existed in Sn-USY. For TS-1, an intense absorption band at 202 nm, which attributed to the presence of framework Ti^{4+} with tetrahedral coordination, is observed [34]. Furthermore, a little absorption band appears at around 313 nm, which is the main absorption band in spectrum of TiO_2 as shown in Fig. 2b, indicating the presence of some aggregated TiO_2. Presence of some TiO_2 is caused by that the Ti content actually applied in the synthesis of TS-1 is slightly higher than the theoretical maximum Ti content can be introduced to the framework (2.5%, molar fraction). Excess Ti was used in the synthesis of TS-1 to ensure the maximum framework Ti content. FT-IR spectroscopy of absorbed base molecules was used to study the acidic properties of samples. As shown in Fig. 3, IR bands at ~ 1447 cm^{-1} observed in the spectra of the TS-1 can be ascribed to pyridine adsorption on Lewis

(L) acid sites [35]. The appearance of band at 1491 cm^{-1} for TS-1 indicates pyridine adsorption on L acid sites [35]. For Sn-β and Sn-USY, the IR band at 1491 cm^{-1} was ascribed to pyridine adsorption on both L and Brønsted (B) acid sites [30, 33]. Both Sn-β and Sn-USY provided the strong absorption band at 1452 cm^{-1}, assigned to the pyridine bound with the L acid Sn sites [30, 33]. The similarity of FT-IR spectra between Sn-β and Sn-USY indicates the similar acid properties between Sn-β and Sn-USY. A very weak absorption feature at 1547 cm^{-1} related to the B acid was also observed in the spectra of Sn-β and Sn-USY [30, 33]. Location of the band at 1447 cm^{-1} for TS-1 is different from the locations of the bands at 1452 cm^{-1} for Sn-β and Sn-USY indicating the different L acid properties of TS-1 from Sn-β and Sn-USY.

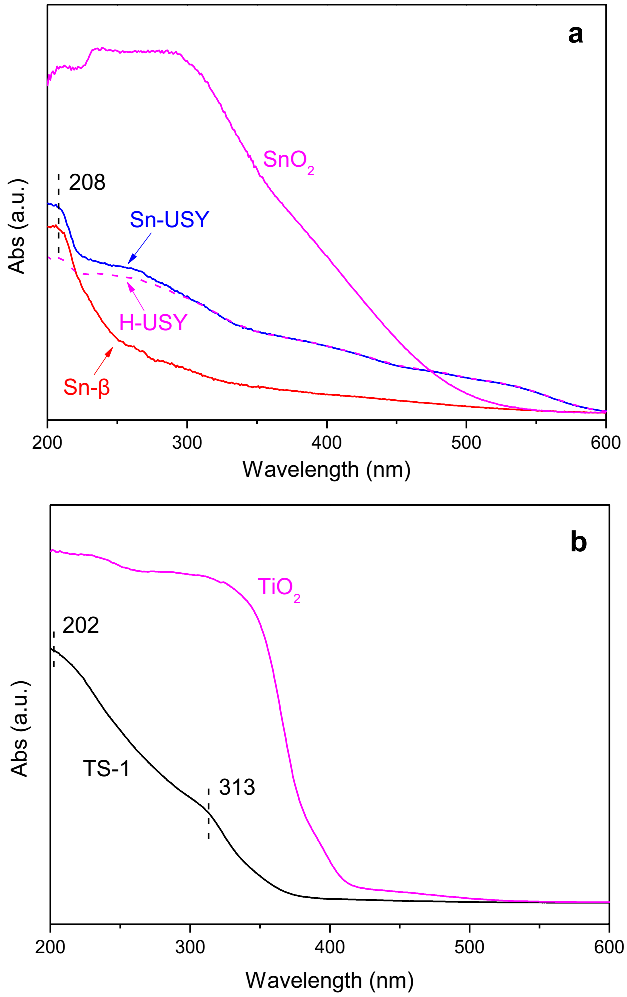

Fig. 2 UV–Vis spectra of Sn-β, Sn-USY, and SnO_2 (**a**), and TS-1, and TiO_2 (**b**)

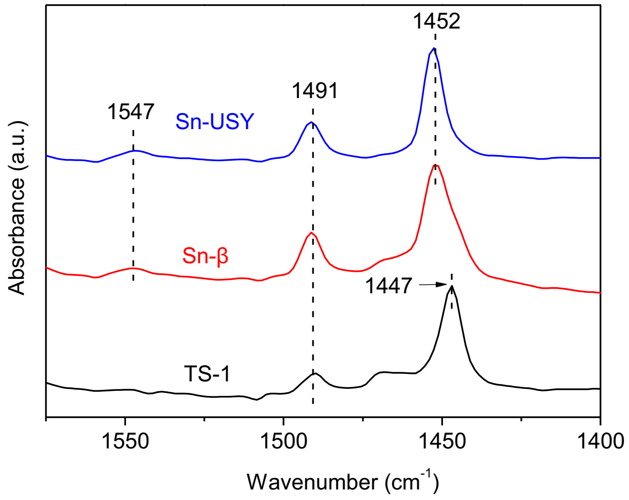

Fig. 3 FT-IR spectra of Sn-β, Sn-USY and TS-1 after pyridine adsorption and evacuation at 150 °C for 30 min

3.2 Catalytic Conversion of DHA to MLA Over Sn-β

As reported in previous literature, both Sn-β and Sn-USY have good catalytic performance on conversion of DHA to MLA in methanol. In this work, Sn-β and Sn-USY were tested as catalyst firstly to compare their catalytic performance in the presence of TS-1 which would be used as oxidative catalyst in the following conversion of MLA to MPA (Table 2). Interestingly, Sn-USY and Sn-β showed the similar catalytic performance. After reaction at 50 °C for 5 h, 85% MLA yield with 100% DHA conversion and 86% MLA yield with 100% DHA conversion were obtained over Sn-USY and Sn-β, respectively. The similarity of the catalytic performance between Sn-USY and Sn-β is caused by their similar acid properties (Fig. 3). In this work, Sn-β was selected as the catalyst for conversion of DHA to MLA in the following study. The reaction includes two successive steps: (1) conversion of DHA to MLA over Sn-β (desired amount of TS-1 was also added at beginning of this step), (2) oxidation of MLA to MPA over TS-1 started by addition of H_2O_2. To simplify the operation, Sn-β and TS-1 were added to the reactor simultaneously at the first step. As shown in Table 2, the addition of TS-1 in the first step does not affect the MLA yield under the same conditions.

Table 2 Catalytic conversion of DHA to MLA over Sn-USY and Sn-β in the presence of TS-1

Sample	Conversion of DHA (%)	Yield of MLA (%)
Sn-USY	100	85
Sn-β	100	86
Sn-β[a]	100	85

Reaction conditions: 5 mL of methanol, 0.2 g of DHA, 0.1 g of TS-1, 0.2 g of Sn containing zeolite (Sn-β or Sn-USY), 50 °C, 5 h

[a] No TS-1 was added

3.3 Conversion of DHA to MPA Over Hybrid Sn-β and TS-1

To get more information about the catalytic performance for Sn-β and TS-1, the effects of reaction conditions including the amount of methanol, amount of Sn-β and TS-1, reaction temperature, amount of H_2O_2, and reaction time were investigated. In this study, 100% DHA conversion were obtained for all the catalytic tests, however, total yield of MLA and MPA was lower than 100% implying the formation of byproducts which was not detected. Figure 4 shows the effect of methanol volume on the conversion of DHA to MPA at 50 °C. When the methanol amount increased from 1 to 2 mL, the yields of MLA and MPA increased. When the methanol was small (<2 mL), methanol cannot totally immerse the solid catalyst and the mass transfer in the slurry of the reaction mixture is poor. With the further increase of the methanol amount to 3.5 mL, MLA yield increased but the MPA yield decreased. This implies that more methanol facilitated the conversion of DHA to MLA, but conversion of MLA to MPA was suppressed. Methanol amount affects the concentration of H_2O_2 which was used as oxidant in the oxidation of MLA to MPA. With the increase of methanol amount, concentration of H_2O_2 would decrease which might lead to the suppression the formation of MPA. As shown in Fig. 4, the yield of MPA reached a maximum of 54% when the methanol volume was 2 mL which was selected in the following study.

The effect of Sn-β amount on the conversion of DHA to MPA is shown in Fig. 5. Sn-β provides the active sites for the conversion of DHA to MLA. Total yield of MLA and MPA reflects the catalytic performance of Sn-β, because formation of MPA was caused by further oxidation of MLA. When the Sn-β amount was increased from 0.1 to 0.4 g, the total yields of MLA and MPA were comparable. 0.3 g of Sn-β was used in the following study, because the yield of MPA reached a maximum of 59% when the Sn-β amount was 0.3 g. Figure 6 shows the effect of TS-1 amount on the conversion of DHA to MPA. Without TS-1, only MLA (78% yield) was obtained and no MPA formed although H_2O_2 was added. This means that Sn-β and TS-1 played distinctively different roles in the conversion of DHA to MPA. Sn-β provides only the active sites for the conversion of DHA to MLA and TS-1

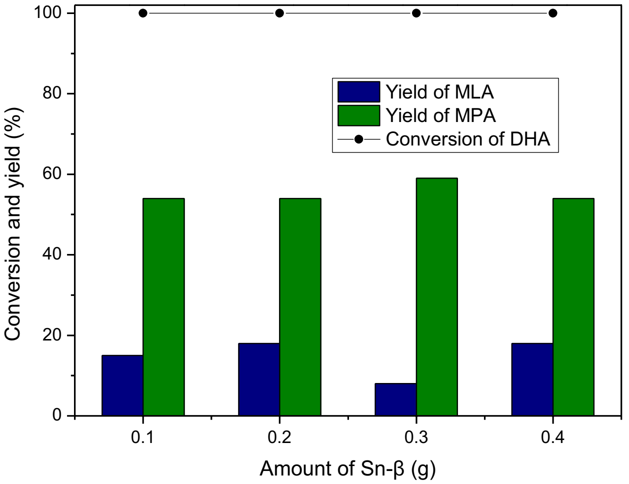

Fig. 5 Effect of Sn-β amount on the conversion of DHA to MPA. Reaction conditions: 2 mL of methanol, 0.2 g of DHA, 0.2 g of TS-1, 2 mL of H_2O_2, 50 °C, reaction time before addition of H_2O_2 was 12 h, reaction time after addition of H_2O_2 was 5 h

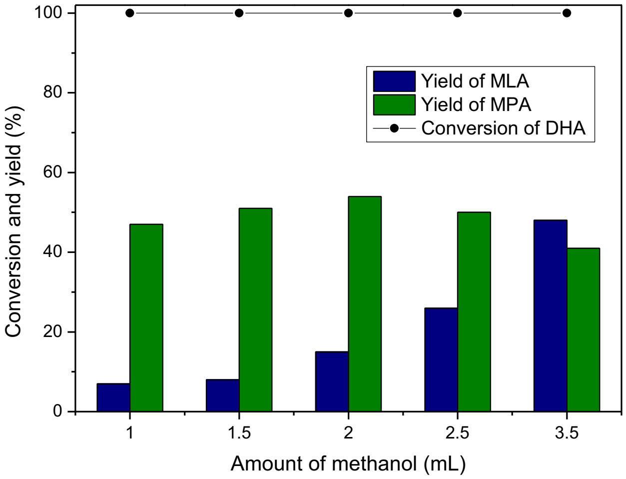

Fig. 4 Effect of methanol amount on the conversion of DHA to MPA. Reaction conditions: 0.2 g of DHA, 0.4 g of Sn-β, 0.2 g of TS-1, 2 mL of H_2O_2, 50 °C, reaction time before addition of H_2O_2 was 12 h, reaction time after addition of H_2O_2 was 5 h

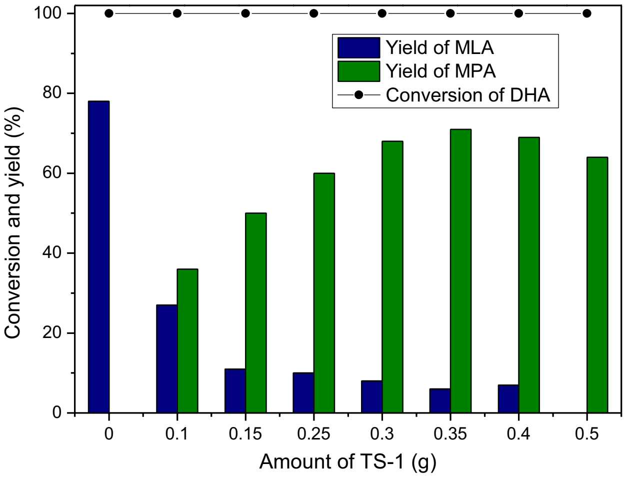

Fig. 6 Effect of TS-1 amount on the conversion of DHA to MPA. Reaction conditions: 2 mL of methanol, 0.2 g of DHA, 0.3 g of Sn-β, 2 mL of H_2O_2, 50 °C, reaction time before addition of H_2O_2 was 12 h, reaction time after addition of H_2O_2 was 5 h

is indispensable for the oxidation of MLA to MPA. Both TS-1 and Sn-β are L acid catalysts, however, the different electronic structure of Ti^{4+} and Sn^{4+} leads to the different active sites in TS-1 and Sn-β (Fig. 3). With the increase of TS-1 amount from 0 to 0.35 g, yield of MLA decreased from 78 to 6% and yield of MPA increased from 0 to 71%. With the increase of TS-1 amount, amount of L acid sites for the conversion of MLA to MPA increased, and this is favorable for the conversion of MLA to MPA. Further increased the TS-1 amount to 0.5 g, all the MLA converted to MPA. However, yield of MPA decreased to 64%. When TS-1 amount is too large, contact between Sn-β and DHA would be hindered because of the adsorption of DHA on TS-1 leading to the decrease of the catalytic activity of Sn-β. This futher caused the decrease of the MPA yield. Thus, 0.35 g of TS-1 was selected in the following study. Based on the reaction scheme for the conversion of DHA to MLA over Sn-β proposed in the literature and the scheme for the oxidation of MLA to MPA over TS-1 illustrated in our previous report [13, 15, 25, 26], the reaction scheme for the conversion of DHA to MPA in methanol over Sn-β and TS-1 was proposed (Scheme 1). Firstly, pyruvic aldehyde (PA) forms by dehydration of DHA and/or glyceraldehyde (GLA) over B and/or L acid sites of Sn-Beta. Then, isomerization and alcohol-addition of PA lead to the formation of MLA over L acid sites of Sn-Beta. When the H_2O_2 is added to the reactor, Ti(OOH) species form on the surface of TS-1. The MLA desorbs from the Sn-Beta, and adsorbs on TS-1. The hydroxyl group of MLA reacts with Ti(OOH) leading to dehydration. After that, desorption of MPA from TS-1 occurs, and TS-1 is recovered. This reaction pathway explains the roles of Sn-β, TS-1 and H_2O_2 in this reaction. As listed in Table 2, further conversion of MLA cannot proceed without H_2O_2 leading to the high yield of MLA. When the H_2O_2 was added, oxidation of MLA to MPA would occur in presence of Ti(OOH). In this case, yield of MLA decreased and yield of MPA increased. As mentioned above, side reactions occurred in this catalytic system. For conversion of DHA to MLA, the by-products might be the condensation and/or polymerization products of the DHA and the intermediates [15, 25, 26]. Detection of these by-products by GC is difficult. This might be why conversions of DHA are 100%, but yields of MLA are about 85% in Table 2. However, for most reactions after addition of H_2O_2, total yield of MPA and MLA is lower than 80%. This implies that there is side reaction in the oxidation of MLA. We had proved in previous work that MPA is unstable

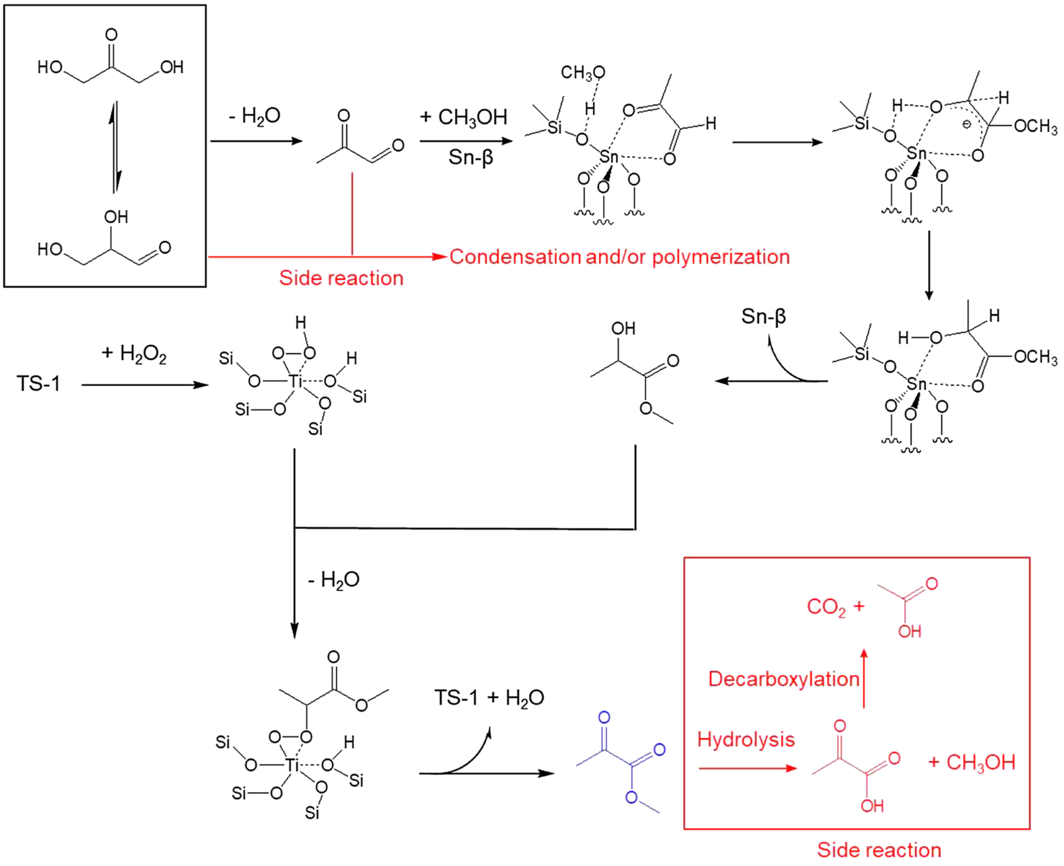

Scheme 1 Proposed reaction scheme for the conversion of DHA to MPA over Sn-β and TS-1

[13]. In the presence of H_2O_2, decomposition of MPA might occur through hydrolysis and decarboxylation (Scheme 1).

H_2O_2 is the oxidant for the oxidation of MLA to MPA. Effect of H_2O_2 amount on the conversion of DHA to MPA is shown in Fig. 7. When the 0.5 mL of H_2O_2 was applied, yields of MLA and MPA were 43% and 40%, respectively. This indicates that the oxidation of MLA is insufficient. Theoretically, 0.11 mL of H_2O_2 can realize the complete conversion of 0.2 g of DHA to MPA. However, 2 mL of methanol was used as solvent in the reaction, and the added H_2O_2 aqueous would be diluted. Lower addition amount of H_2O_2 leads to the lower concentration of H_2O_2 in the reaction solution. Oxidation ability of H_2O_2 is related to the concentration. That is why MLA yield decreased to 6% and MPA yield increased to 71% when the H_2O_2 amount increased from 0.5 to 2 mL. Further increased the amount of H_2O_2 to 3 mL would lead to the decrease of the MPA yield. Besides increase the H_2O_2 concentration in the reaction mixture, the increase of the addition amount of H_2O_2 also leads to the increase of the total volume of the reaction mixture, and this would cause the decrease of the concentration of reactants and intermediates. Increase of H_2O_2 concentration and decrease of the reactants and intermediates concentration are two contrary factors for the conversion of DHA to MPA. When the amount of H_2O_2 is in the range of 2–3 mL, decrease of the reactants and intermediates concentration is the major factor which caused the decrease of the MPA yield.

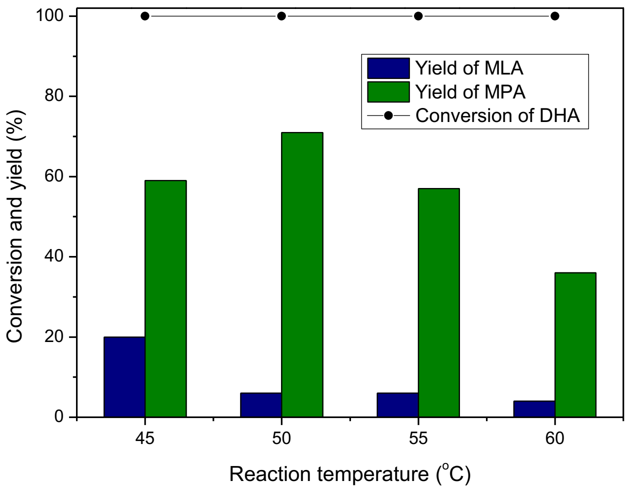

Fig. 8 Effect of reaction temperature on the conversion of DHA to MPA. Reaction conditions: 2 mL of methanol, 0.2 g of DHA, 0.3 g of Sn-β, 0.35 g of TS-1, 2 mL of H_2O_2, reaction time before addition of H_2O_2 was 12 h, reaction time after addition of H_2O_2 was 5 h

Reaction temperature and reaction time were optimized. Figure 8 shows effect of the reaction temperature on the conversion of DHA to MPA. This reaction is very sensitive to the reaction temperature. When the reaction temperature increased from 45 to 50 °C, the MLA yield decreased from 20% to 6%, and the MPA yield increased from 59% to 71%. Further elevated the temperature, the MPA yield decreased, which might be caused by the instability of MPA. We had proved that decomposition of MPA would occur through hydrolysis and decarboxylation in the presence of H_2O_2 [13]. As shown in Fig. 9, with the increase of the reaction time before addition of H_2O_2 from 1 to 5 h, MLA yield kept comparable, and MPA yield increased from 35% to 69%. Further increased the reaction time to 12 h, MPA yield increased slightly to 71%. Thus,

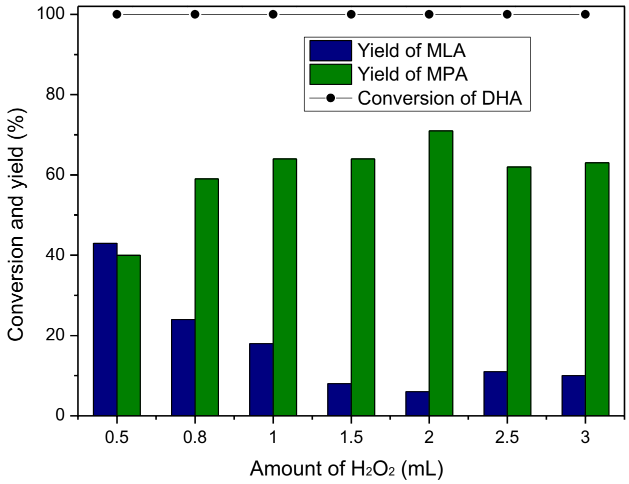

Fig. 7 Effect of H_2O_2 amount on the conversion of DHA to MPA. Reaction conditions: 2 mL of methanol, 0.2 g of DHA, 0.3 g of Sn-β, 0.35 g of TS-1, 50 °C, reaction time before addition of H_2O_2 was 12 h, reaction time after addition of H_2O_2 was 5 h

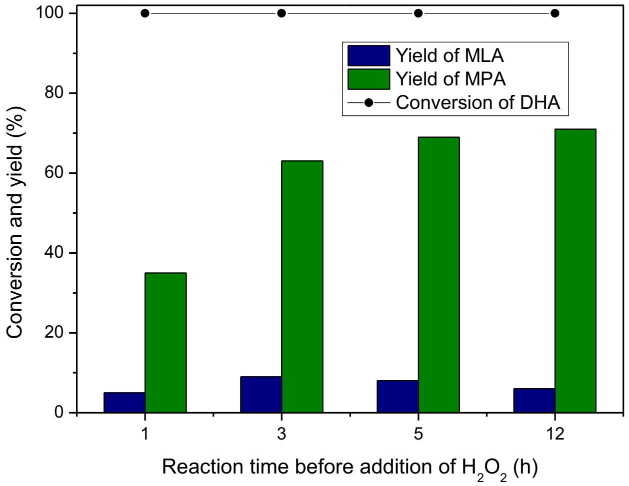

Fig. 9 Effect of the reaction time before addition of H_2O_2 on the conversion of DHA to MPA. Reaction condition: 2 mL of methanol, 0.2 g of DHA, 0.3 g of Sn-β, 0.35 g of TS-1, 2 mL of H_2O_2, 50 °C, reaction time after addition of H_2O_2 was 5 h

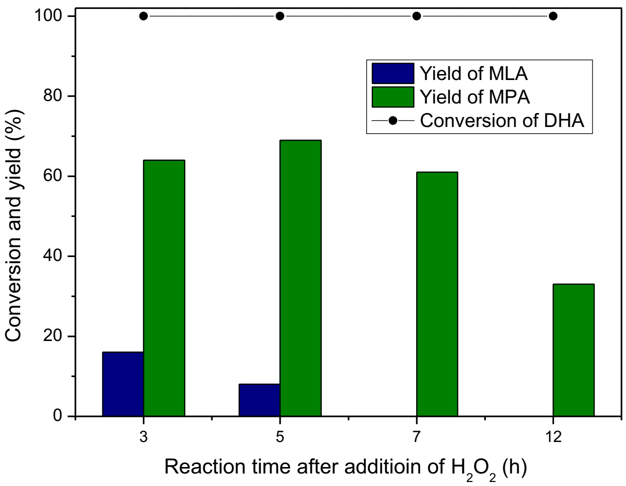

Fig. 10 Effect of the reaction time after addition of H_2O_2 on the conversion of DHA to MPA. Reaction condition: 2 mL of methanol, 0.2 g of DHA, 0.3 g of Sn-β, 0.35 g of TS-1, 2 mL of H_2O_2, 50 °C, reaction time before addition of H_2O_2 was 5 h

before addition of H_2O_2, there must be enough reaction time (≥ 5 h) for the conversion of DHA to MLA. Figure 10 shows the effect of reaction time after addition of H_2O_2. For this step, when the reaction time is shorter, for example 3 h, oxidation of MLA to MPA would be insufficient. When the reaction time is longer, for example ≥ 7 h, MLA can be oxidized to MPA completely, however, decrease of MPA yield would occur because the MPA is unstable.

4 Conclusions

MPA was synthesized from DHA over Sn-β and TS-1 hybrid molecular sieves at low temperature. Sn-β and TS-1 provide the active sites for conversion of DHA to MLA and oxidation of MLA to MPA, respectively. Synergism of Lewis acid sites on Sn-β and TS-1 realize the production of MPA from DHA. After optimization, 71% yield of MPA can be obtained under 50 °C. This is the first report for the synthesis of MPA from DHA directly, and this work will contribute to the green utilization of glycerol.

Acknowledgements We are grateful to the National Natural Science Foundation of China (Grant Nos. 21802125, 21875222, 21871236), China Postdoctoral Science Foundation (Grant No. 2017M612418), the fund of the State Key Laboratory of Catalysis in DICP (Grant No. N-16-02), the Henan Science and Technology Project (Grant No. 172102210490) and Program of Processing and Efficient Utilization of Biomass Resources of Henan Center for Outstanding Overseas Scientists (Grant No. GZS2018004) for the financial supports.

Compliance with Ethical Standards

Conflict of interest The authors declare that they have no conflict of interest.

References

1. Bozkurt F, Tornuk F, Toker OS, Karasu S, Arici M, Durak MZ (2016) Effect of vaporized ethyl pyruvate as a novel preservation agent for control of postharvest quality and fungal damage of strawberry and cherry fruits. LWT Food Sci Technol 65:1044–1049. https://doi.org/10.1016/j.lwt.2015.09.043
2. Wang Y, Lewis JD, Román-Leshkov Y (2016) Synthesis of itaconic acid ester analogues via self-aldol condensation of ethyl pyruvate catalyzed by hafnium BEA zeolites. ACS Catal 6:2739–2744. https://doi.org/10.1021/acscatal.6b00561
3. Dusselier M, Wouwe PV, Dewaele A, Makshina E, Sels BF (2013) Lactic acid as a platform chemical in the biobased economy: the role of chemocatalysis. Energy Environ Sci 6:1415–1442. https://doi.org/10.1039/C3EE00069A
4. Hernández K, Gómez A, Joglar J, Bujons J, Parella T, Clapés P (2017) 2-Keto-3-deoxy-$_L$-rhamnonate aldolase (YfaU) as catalyst in aldol additions of pyruvate to amino aldehyde derivatives. Adv Synth Catal 359:2090–2100. https://doi.org/10.1002/adsc.201700360
5. Zhang B, Zhu Y, Zhang J, Wang D, Sun L, Hong J (2017) Engineered *Kluyveromyces marxianus* for pyruvate production at elevated temperature with simultaneous consumption of xylose and glucose. Bioresour Technol 224:553–562. https://doi.org/10.1016/j.biortech.2016.11.110
6. Zhang W, Innocenti G, Oulego P, Gitis V, Wu H, Ensing B, Cavani F, Rothenberg G, Shiju NR (2018) Highly selective oxidation of ethyl lactate to ethyl pyruvate catalyzed by mesoporous vanadia–titania. ACS Catal 8:2365–2374. https://doi.org/10.1021/acscatal.7b03843
7. Zhang L, Wang R, Song L, Zhao X, Fan Q, Li H, Yu Q, Li X, Zeng J, Zhang C, Liu T, Wang Z (2019) Aerobic oxidative dehydrogenation of ethyl lactate over reduced $MoVNbO_x$ catalysts. Catal Lett 149:840–850. https://doi.org/10.1007/s10562-018-2616-9
8. Liu K, Huang X, Pidko EA, Hensen EJM (2017) MoO_3–TiO_2 synergy in oxidative dehydrogenation of lactic acid to pyruvic acid. Green Chem 19:3014–3022. https://doi.org/10.1039/C7GC00807D
9. Zhao X, Zhang C, Xu C, Li H, Huang H, Song L, Li X (2016) Kinetics study for the oxidative dehydrogenation of ethyl lactate to ethyl pyruvate over $MoVNbO_x$ based catalysts. Chem Eng J 296:217–224. https://doi.org/10.1016/j.cej.2016.03.088
10. Hayashi H, Sugiyama S, Katayama Y, Sakai K, Sugino M, Shigemoto N (1993) Liquid-phase oxidation of ethyl lactate to pyruvate over suspended oxide catalysts. J Mol Catal 83:207–217. https://doi.org/10.1016/0304-5102(93)87020-9
11. Sugiyama S, Kikumoto T, Tanaka H, Nakagawa K, Sotowa KI, Maehara K, Himeno Y, Ninomiya W (2009) Enhancement of catalytic activity on Pd/C and Te-Pd/C during the oxidative dehydrogenation of sodium lactate to pyruvate in an aqueous phase under pressurized oxygen. Catal Lett 131:129–134. https://doi.org/10.1007/s10562-009-9920-3
12. Zhang C, Wang T, Ding Y (2017) Oxidative dehydrogenation of lactic acid to pyruvic acid over Pb–Pt bimetallic supported on carbon materials. Appl Catal A 533:59–65. https://doi.org/10.1016/j.apcata.2017.01.010
13. Lu T, Zou J, Zhan Y, Yang X, Wen Y, Wang X, Zhou L, Xu J (2018) Highly efficient oxidation of ethyl lactate to ethyl pyruvate

catalyzed by TS-1 under mild conditions. ACS Catal 8:1287–1296. https://doi.org/10.1021/acscatal.7b03558

14. Skaf DW, Natrin NG, Brodwater KC, Bongo CR (2012) Comparison of phototcatalytic hydrogen production from glycerol and crude glycerol obtained from biodiesel processing. Catal Lett 142:1175–1179. https://doi.org/10.1007/s10562-012-0886-1
15. Lu T, Fu X, Zhou L, Su Y, Yang X, Han L, Wang J, Song C (2017) Promotion effect of Sn on Au/Sn-USY catalysts for one-pot conversion of glycerol to methyl lactate. ACS Catal 7:7274–7284. https://doi.org/10.1021/acscatal.7b02254
16. Zhou L, Xu Y, Yang X, Lu T, Han L (2019) Utilization of biodiesel byproduct glycerol: production of methyl lactate over Au/CuO and Sn-Beta binary catalyst under mild reaction conditions. Energ Convers Manage 196:277–285. https://doi.org/10.1016/j.enconman.2019.06.011
17. Wang X, Wu G, Wang F, Ding K, Zhang F, Liu X, Xue Y (2012) Base-free selective oxidation of glycerol with 3% H_2O_2 catalyzed by sulphonato–salen–chromium(III) intercalated LDH. Catal Commun 28:73–76. https://doi.org/10.1016/j.catcom.2012.08.014
18. Rodrigues EG, Carabineiro SAC, Chen X, Delgado JJ, Figueiredo JL, Pereira MFR (2011) Selective oxidation of glycerol catalyzed by Rh/activated carbon: importance of support surface chemistry. Catal Lett 141:420–431. https://doi.org/10.1007/s10562-010-0515-9
19. Ning X, Li Y, Yu H, Peng F, Wang H, Yang Y (2016) Promoting role of bismuth and antimony on Pt catalysts for the selective oxidation of glycerol to dihydroxyacetone. J Catal 335:95–104. https://doi.org/10.1016/j.jcat.2015.12.020
20. Lee S, Kim HJ, Lim EJ, Kim Y, Noh Y, Huber GW, Kim WB (2016) Highly selective transformation of glycerol to dihydroxyacetone without using oxidants by a PtSb/C-catalyzed electrooxidation process. Green Chem 18:2877–2887. https://doi.org/10.1039/C5GC02865E
21. Liu SS, Sun KQ, Xu BQ (2014) Specific selectivity of Au-catalyzed oxidation of glycerol and other C_3-polyols in water without the presence of a base. ACS Catal 4:2226–2230. https://doi.org/10.1021/cs5005568
22. Oberhauser W, Evangelisti C, Caporali S, Santo VD, Bossola F, Vizza F (2017) Ethyl lactate from dihydroxyacetone by a montmorillonite-supported Pt(II) diphosphane complex. J Catal 350:133–140. https://doi.org/10.1016/j.jcat.2017.04.006
23. Hayashi H, Shigemoto N, Sugiyama S, Masaoka N, Saitoh K (1993) X-ray photoelectron spectra for the oxidation state of TeO_2–MoO_3 catalyst in the vapor-phase selective oxidation of ethyl lactate to pyruvate. Catal Lett 19:273–277. https://doi.org/10.1007/BF00771764
24. Godard N, Collard X, Vivian A, Bivona LA, Fiorilli S, Fusaro L, Aprile C (2018) Rapid room temperature synthesis of tin-based mesoporous solids: influence of the particle size on the production of ethyl lactate. Appl Catal A 556:73–80. https://doi.org/10.1016/j.apcata.2018.02.014
25. Wang X, Liang F, Huang C, Li Y, Chen B (2016) Siliceous tin phosphates as effective bifunctional catalysts for selective conversion of dihydroxyacetone to lactic acid. Catal Sci Technol 6:6551–6560. https://doi.org/10.1039/C6CY00553E
26. Pighin E, Díez VK, Di Cosimo JI (2017) Kinetic study of the ethyl lactate synthesis from triose sugars on Sn/Al_2O_3 catalysts. Catal Today 289:29–37. https://doi.org/10.1016/j.cattod.2016.10.002
27. Guo Q, Fan DF, Pidko DEA, Graaff WNP, Feng PDZ, Li PDC, Hensen PDEM (2013) Highly active and recyclable Sn-MWW zeolite catalyst sugar conversion to methyl lactate and lactic acid. Chemsuschem 6:1352–1356. https://doi.org/10.1002/cssc.201300160
28. Zhu Z, Xu H, Jiang J, Guan Y, Wu P (2017) Sn-Beta zeolite hydrothermally synthesized via interzeolite transformation as efficient Lewis acid catalyst. J Catal 352:1–12. https://doi.org/10.1016/j.jcat.2017.04.031
29. Yao JK, Fu KR, Wang YC, Li TD, Liu HX, Wang JG (2017) Hierarchically porous Sn-β-zeolites via an OSDA-free synthesis. Green Chem 19:3214–3218. https://doi.org/10.1039/C7GC01040K
30. Dijkmans J, Dusselier M, Gabriëls D, Houthoofd K, Magusin PCMM, Huang S, Pontikes Y, Trekels M, Vantomme A, Giebeler L, Oswald S, Sels BF (2015) Cooperative catalysis for multistep biomass conversion with Sn/Al beta zeolite. ACS Catal 5:928–940. https://doi.org/10.1021/cs501388e
31. Osmundsen CM, Holm MS, Dahl S, Taarning E (2012) Tin-containing silicates: structure–activity relations. Proc R Soc A 468:2000–2016. https://doi.org/10.1098/rspa.2012.0047
32. Yang X, Wu L, Wang Z, Bian J, Lu T, Zhou L, Chen C, Xu J (2016) Conversion of dihydroxyacetone to methyl lactate catalyzed by highly active hierarchical Sn-USY at room temperature. Catal Sci Technol 6:1757–1763. https://doi.org/10.1039/C5CY01037C
33. Dijkmans J, Gabriëls D, Dusselier M, Clippel F, Vanelderen P, Houthoofd K, Malfliet A, Pontikes Y, Sels BF (2013) Productive sugar isomerization with highly active Sn in dealuminated β zeolites. Green Chem 15:2777–2785. https://doi.org/10.1039/C3GC41239C
34. Maurelli S, Vishnuvarthan M, Chiesa M, Berlier G, Doorslaer SV (2011) Elucidating the nature and reactivity of Ti ions incorporated in the framework of AIPO-5 molecular sieves. New evidence from ^{31}PHYSCORE spectroscopy. J Am Chem Soc 133:7340–7343. https://doi.org/10.1021/ja202210g
35. Bonino F, Damin A, Bordiga S, Lamberti C, Zecchina A (2003) Interaction of CD_3CN and pyridine with the Ti(IV) centers of TS-1 catalysts: a spectroscopic and computational study. Langmuir 19:2155–2161. https://doi.org/10.1021/la0262194